17th World Conference on Earthquake Engineering, 17WCEE
Sendai, Japan - September 13th to 18th 2020

NOVEL TRANSVERSE PUSHOVER ANALYSIS METHOD FOR CONCRETE TOWER OF LONG-SPAN CABLE-STAYED BRIDGE

J. Wang[1], A. Ye [2], X. Wang[3]

[1] *Ph.D. Candidate, Tongji University, jc_wang@tongji.edu.cn*
[2] *Professor, Ph.D., Tongji University, yeaijun@tongji.edu.cn (corresponding author)*
[3] *Ph.D., Hohai University, x.wang@hhu.edu.cn*

Abstract

The tower of a long-span cable-stayed bridge is the paramount component for reliable load transmission. Conventional seismic analysis methods like Incremental Dynamic Analysis (IDA), Modal Pushover Analysis (MPA) and Adaptive Pushover Analysis (APA) show different levels of limitations when utilized in towers of long-span bridges. To efficiently obtain seismic demands and identify seismic failure mechanisms of the towers as well as quantifying their ductile behavior, a novel Deformation-based Pushover Analysis (DPA) method, which is based on the well-known Equal Displacement Principle, is proposed in this paper. This method starts with an elastic response-spectrum analysis on the elastic full-bridge model at a low seismic intensity to obtain the deformation-shape of the bridge tower, which is employed as the load-pattern for the following pushover analysis on the nonlinear singer-tower model. The proposed method is then applied to quantify seismic behavior of the concrete tower of an as-built long-span cable-stayed bridge, the Sutong Bridge, under selected ground motions. Also, IDA is applied as the reference to verify the proposed DPA method. The results show that (1) DPA method can efficiently predict seismic demands of long-span bridge towers with reasonable accuracy for engineering practice, and (2) DPA is able to predict the failure process of bridge towers and provide conservative results on peak horizontal force and displacement ductility.

Keywords: long-span cable-stayed bridge tower, seismic analysis method, IDA, Deformation-based Pushover Analysis

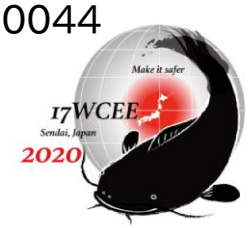

1. Introduction

The tower of a long-span cable-stayed bridge is the paramount component for reliable load transmission. For this reason, existing seismic design codes often give preference to the elastic design of the towers [1-3], which inevitably causes a large demand of reinforcements in concrete towers. This issue is obviously buckling the trend of economical and sustainable construction in this era. On the other hand, tower-deck connections are often designed fixed in the transverse direction for the purpose of operational stability [4]. This renders an incredible transverse seismic demand on the tower, which further aggravates the large demand of reinforcements if the elastic design philosophy is persisted. Nevertheless, constructed long-span cable stayed bridges following the elastic design philosophy for their concrete towers are still vulnerable under strong earthquakes. A noted example is the damage to Ji Lu Bridge in the 1999 Chi-Chi earthquake [5], where the bottom of tower practically yielded [6]. Undoubtedly, in-depth researches on the inelastic behavior of concrete towers under earthquakes are of significant urgency and importance. Accordingly, associated analysis methods are essential tools for the researches.

However, seismic analysis methods for structural evaluation proposed by previous studies show different levels of limitations when utilized in towers of long-span bridges. First of all, the well-known Incremental Dynamic Analysis (IDA) proposed by Bertero in 1977 [7,8] is generally deemed an accurate method, despite extensive computational efforts are demanded when employed in long-span bridge structures, where the numerical models often involve thousands of nodes and elements with high levels of geometric and material nonlinearities. To simplify the analysis procedure, different nonlinear pushover analysis methods have been introduced in recent years. The Modal Pushover Analysis (MPA) [9,10] developed by Chopra and Goel in 2002 is ease of use as seismic demands are simply determined by combining several dominant modal demands. Nevertheless, MPA cannot take damage accumulation and modal parameters variation into account, thus failing to provide reasonable inelastic results when applied to complex structures like towers of long-span bridges. Another widely-adopted pushover analysis is the Adaptive Pushover Analysis (APA) [11-13], where load distribution is evaluated step-by-step as a function of updated modal characteristics of the structure. Nonetheless, APA cannot justify its application in long-span bridge towers due to the highly complex algorithms and computational demands which are even comparable to conventional nonlinear time-history analysis.

In order to efficiently and accurately predict the seismic demands, especially the inelastic behavior, of towers in long-span bridges for engineering practice, a Deformation-based Pushover Analysis (DPA) method is proposed in this paper. Based on the Equal Displacement Principle [14,15], the key idea of DPA is to use easily captured elastic deformation-shape as the stable load-pattern in displacement-based nonlinear pushover analysis. DPA has an overwhelming advantage over IDA and APA in computational efficiency, providing more stable and reasonable inelastic results compared with MPA at the same time due to the validity of Equal Displacement Principle for long-span bridge towers. The proposed DPA is detailed first, followed by a case study to reveal the applicability of the proposed DPA method by comparing elastoplastic seismic demands of a real concrete long-span bridge tower between DPA and IDA.

2. Proposed Deformation-based Pushover Analysis (DPA) method

The proposed DPA method is based on the widely acknowledged Equal Displacement Principle for intermediate and long-period structures where inelastic displacement demands of flexural structures are generally equal to their elastic demands [14,15]. For long-period structures like cable-stayed bridge towers, it can be considered that they follow the Equal Displacement Principle within limited ductile ranges. Accordingly, the easily captured elastic deformation-shape of the bridge tower is a reasonable displacement-based load-pattern in pushover analysis to assess its elastoplastic performance under earthquakes.

More specifically, the key idea of DPA is to leverage the elastic deformation-shape, which can be readily obtained by a response-spectrum analysis of an elastic full-bridge numerical model (such a model is

often available for the design of the bridge), as the load-pattern for pushover analysis of a nonlinear single-tower model. Fig.1 illustrates the flow chart of the proposed DPA method, including three main steps:

STEP I: Establish the elastic full-bridge numerical model based on commercial finite element software (e.g., SAP2000 [16] or OpenSees [17]), followed by a gravity analysis to ensure the as-built condition. An equivalent nonlinear single-tower model is then built in OpenSees [17] based on the full-bridge model following Wang et al. [18].

STEP II: Perform response spectrum analyses on the elastic full-bridge model at a low intensity (e.g., peak ground acceleration (PGA) = 0.1g) and the elastic deformation-shape of the bridge tower at this intensity are obtained, which are then applied as the stable load-pattern for displacement-based pushover analysis in Step III. It should be noted that the stability of load-pattern is verified before in advance.

STEP III: Scale the obtained load-pattern to target intensities (e.g., different levels of PGA) and impose them on corresponding nodes of the equivalent nonlinear single-tower. Perform displacement-based incremental pushover analysis until the ultimate-state of the tower is reached.

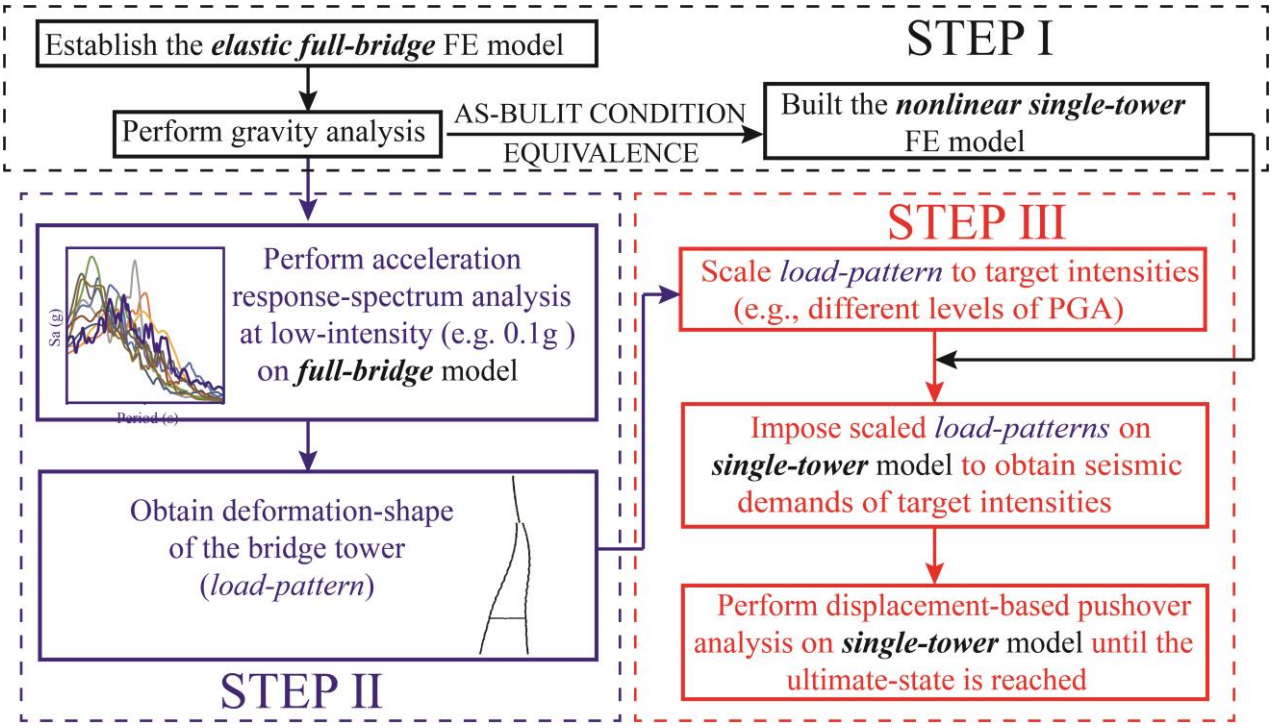

Fig. 1 –Basic procedures of DPA

3. Case study and numerical model

3.1 Case study considered

The Sutong Bridge, a typical kilometer-span cable-stayed bridge, is considered as the case study. The main span of it is up to 1088m with side span of 500m (300+100+100m) on both sides. The total height of two reinforced concrete inverted Y-shaped towers are 300.4m, including 59m and 155m for lower column and middle column separately. The orthotropic steel box girder (41m in width and 4m in height) is supported by two inclined semi-fan cable-planes radiating from the top of bridge towers. Pile-cap foundation is adopted for towers, transition and auxiliary piers. To satisfy the stiffness demand for traffic and wind loads,

transversely fixed bearings and wind-resistant bearings are placed at the deck-pier and deck-tower connections respectively. More details about the Sutong Bridge can be found in [19].

3.2 Numerical modeling and validation

Based on OpenSees, the elastic three-dimensional full-bridge model of the Sutong bridge is established, as shown in Fig.2. Elastic-Beam-Column elements are used to model the deck, tower columns, tower crossbeams and piers. Two-Node-Link element, hardening material model (for longitudinal direction) and Elastic material model (for transverse and vertical directions) are adopted for the modelling of bearings, related parameters of which are also listed in Fig.2. Cables are modelled by truss elements, assigned with initial strains to simulate the as-built condition. To take sag effects into account, the modulus of elasticity of cable elements are modified. The pile-soil-structure interaction is not considered for the simplicity of modelling and subsequent analysis. In other words, piers and towers are simply base-fixed.

PARAMETERS FOR BEARINGS

PIER #	LONGITUDINAL			TRANSVERSE	VERTICAL
	E (Mpa)	Y (kN)	h	E (Mpa)	E (Mpa)
TP1 TP2	25	50	10^{-5}	10^{7}	10^{7}
AP1 AP3	45	90	10^{-5}	10^{7}	10^{7}
AP2 AP4	69	138	10^{-5}	10^{7}	10^{7}

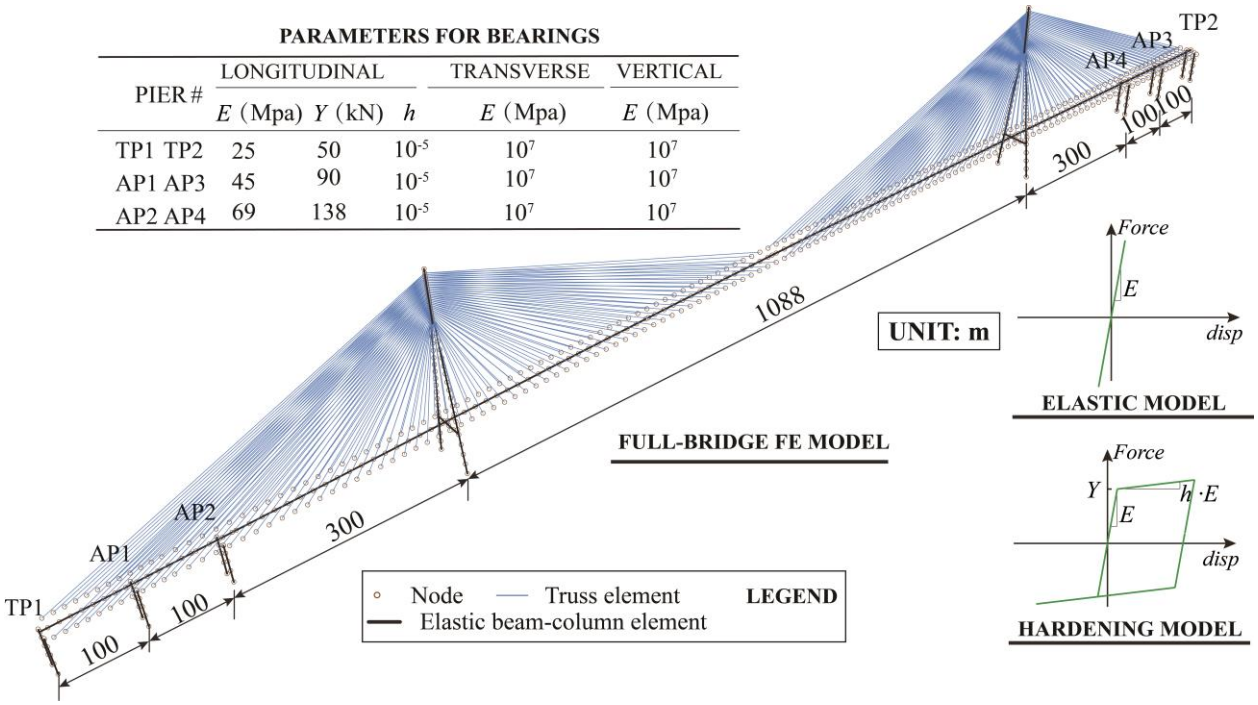

Fig. 2 –Schematic illustration of elastic full-bridge finite element modelling of the Sutong Bridge

A nonlinear single-tower model is then built in OpenSees, as depicted in Fig.3, based on the nonlinear full-bridge model following Wang et al. [18]. The vertically upper column and crossbeam of the tower are modeled by Elastic-Beam-Column elements as they are always elastic-designed (i.e., reinforced by massive prestressed rebars). The displacement-based beam-column elements (15m in depth, 5 integration points for each element) with fiber sections are adopted to represent inclined column sections considering the effect of material nonlinearity and force-moment interaction. The concrete and rebar fibers are modeled by the Kent-Scott-Park model and bilinear model separately. Related modelling parameters are also listed in Fig.3. To account for P-Δ effort, the Corotational Transformation command in OpenSees is employed. The axial forces derived from cables on the tower top are obtained by the gravity analysis of the elastic full-bridge model mentioned before and applied to the corresponding node of the sing-tower model to ensure the as-built condition.

To verify the equivalency between the elastic full-bridge model and the nonlinear single-tower model, the comparation of inner forces along the towers are performed [20]. The results show that they coincide well with each other in terms of axial, shear and bending moments under the dead-load state. Accordingly, pushover analysis in Step III can be conducted on the single-tower model.

It worth noting that IDA, which is applied as reference to verify DPA, is performed on the nonlinear full-bridge model following Wang et al. [18]

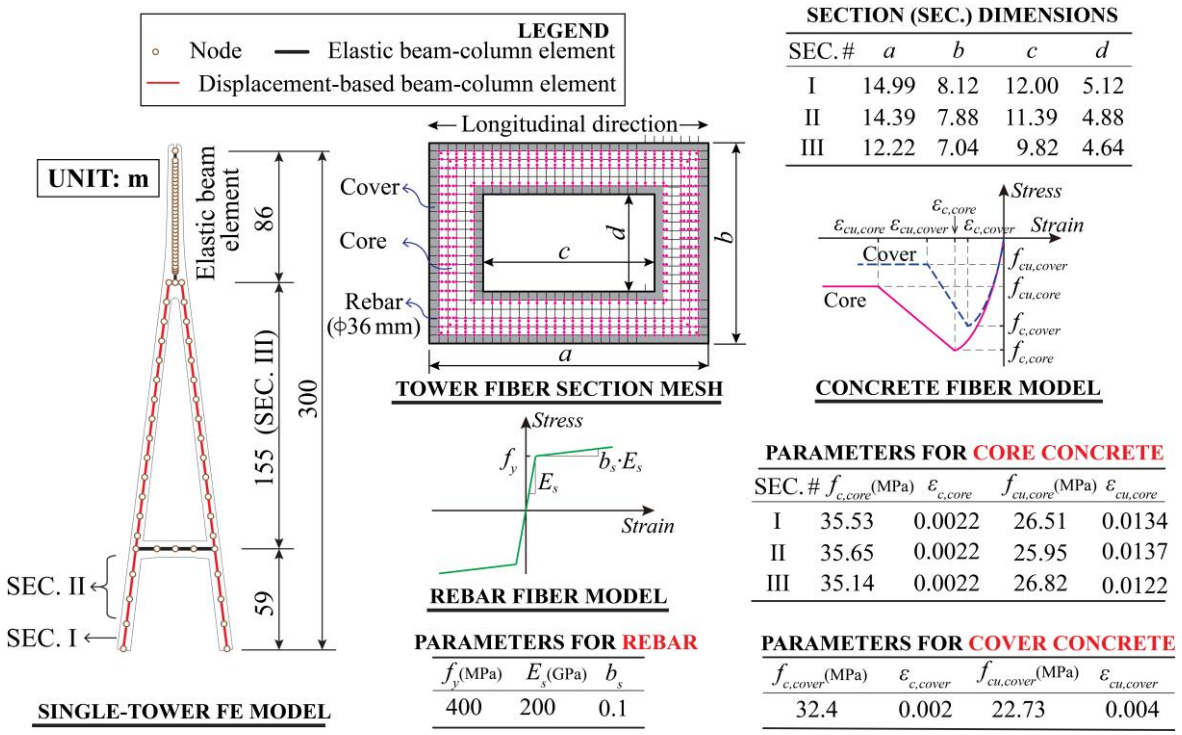

Fig. 3 –Schematic illustration of singer-tower finite element modelling of the tower of Sutong Bridge

3.3 Adopted ground motions

Based on the site condition of Sutong Bridge [21], two ground motion records, Chi-Chi (RSN:1494, Station: TCU054) and Imperial Valley (RSN:0170, Station: EC Country Centre FF), are selected from PEER-NGA strong motion database [22]. Figs. 4 (a) and (b) illustrate their time histories and pseudo-acceleration spectra. In the subsequent IDA procedures, they are scaled from 0.2g with a step of 0.2g until the ultimate-state of the tower is reached. It worth mentioning that the IDA results at other PGAs are determined by linear interpolation. For DPA, the deformation-shape of the tower subjected to selected ground records (PGA 0.1g) are scaled and seismic demands under concerned PGA range (0.01g, 0.02g, 0.03g…, 2.29g, 3g) are obtained from pushover analysis.

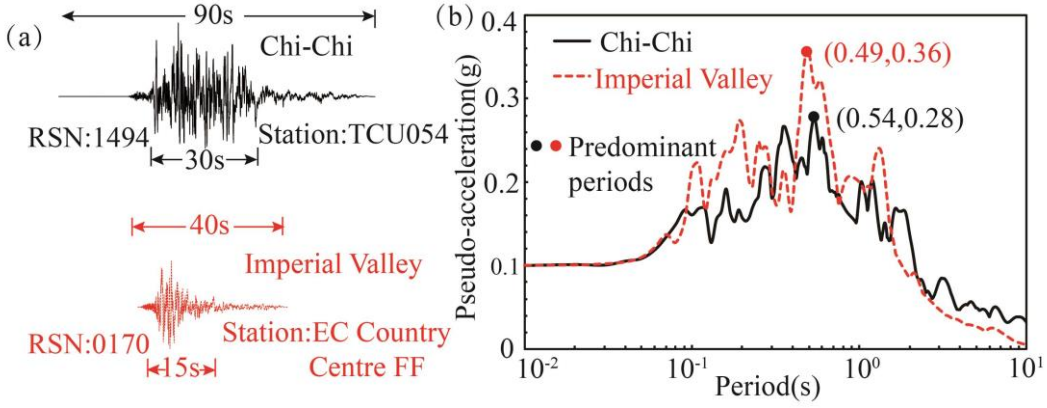

Fig.4-Illustration of acceleration time histories (a) and Pseudo-acceleration spectra (b) of the adopted ground motions scaled to 0.1g

4. Results Interpretation and discussion

4.1 Validation of Equal Displacement Principle

Fig.5(a) displays normalized displacement envelopes of the bridge tower at different levels of PGA by IDA and Response-Spectrum Analysis (RSA). A check on their differences can verify the equal displacement principle. Fig.5(b) shows variations of peak tower-displacement across the studied PGAs and their differences that reflect the error of Equal Displacement Principle. From Fig.5(a), deformation shapes of the tower from IDA remains almost the same with the increase of PGA, quite similar to RSA results, proving the rationality of using the elastic deformation-shape instead of inelastic one as the load-pattern in pushover analysis. Apart from that, it can be seen from Fig.5(b) that elastic displacement demands are quite close to their inelastic counterparts within a certain PGA range (i.e., percentage error within 10%, grey area in Fig.5(b)). It is worth noting that the tower may witness earlier appearance of plastic hinges when subjected to Chi-Chi than Valley as the displacement related to Chi-Chi is larger than that related to Valley under the same PGA.

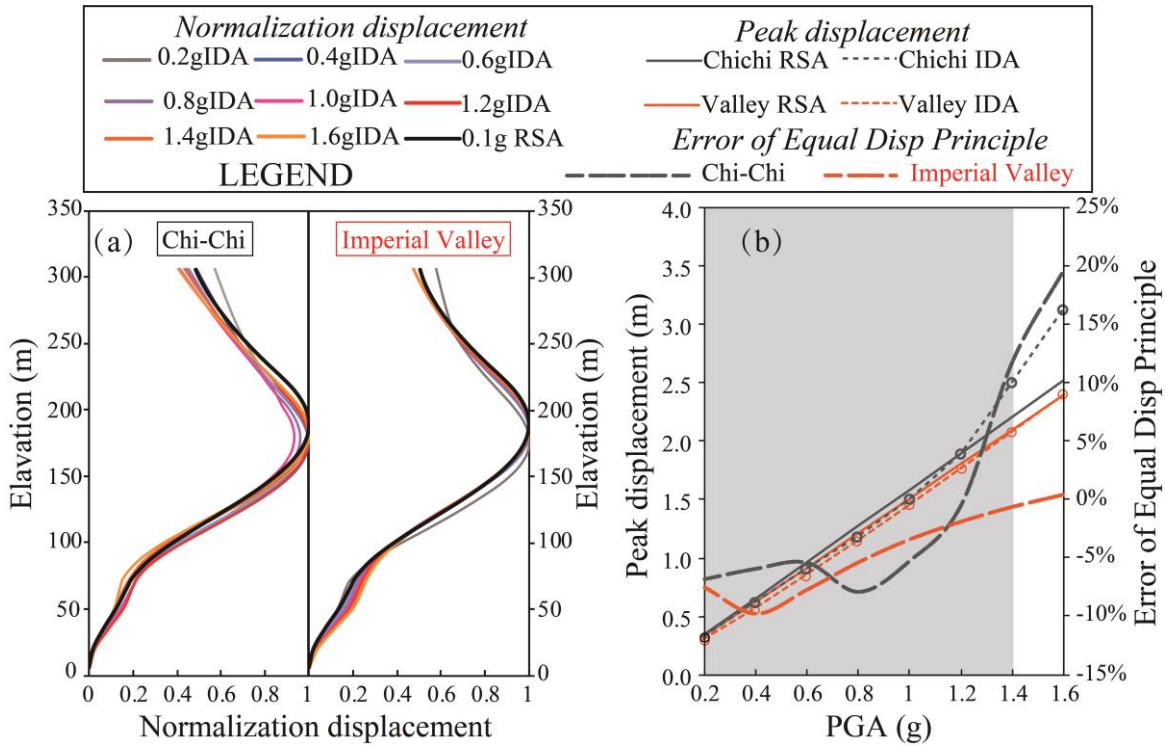

Fig. 5–Normalized displacement envelope (a) and peak displacements (b) of the bridge tower from IDA and RSA; Error of Equal Displacement Principle (b) with the increase of PGA.

4.2 Predicting axial force and moment

Axial force and bending moment are usually highly concerned demand parameters as they are closely related to the judgement of yield- and ultimate-state of the structure as well as the section reinforcement design. Fig.6 illustrates the axial force and bending moment envelope distributions of the bridge tower from IDA and DPA. Table 1 lists the axial force and bending moment in critical sections (the bottom and top of the lower column and the bottom of the middle column, labeled with I, II and III, respectively, in Fig.6) when PGA of Chi-Chi and Imperial Valley is 0.2g, 0.6g, 1.0g and 1.6g, representing the elastic, nearly yield, post-yield and nearly ultimate states, respectively. It can be seen from Fig.6 and Table 1 that DPA can accurately predict the axial force of the bridge tower from the elastic state to nearly ultimate state, especially at the critical sections

with errors within 10%. As for bending moment, errors are less than 25% and 18% when DPA is employed to estimate the elastic and inelastic demands of critical sections respectively.

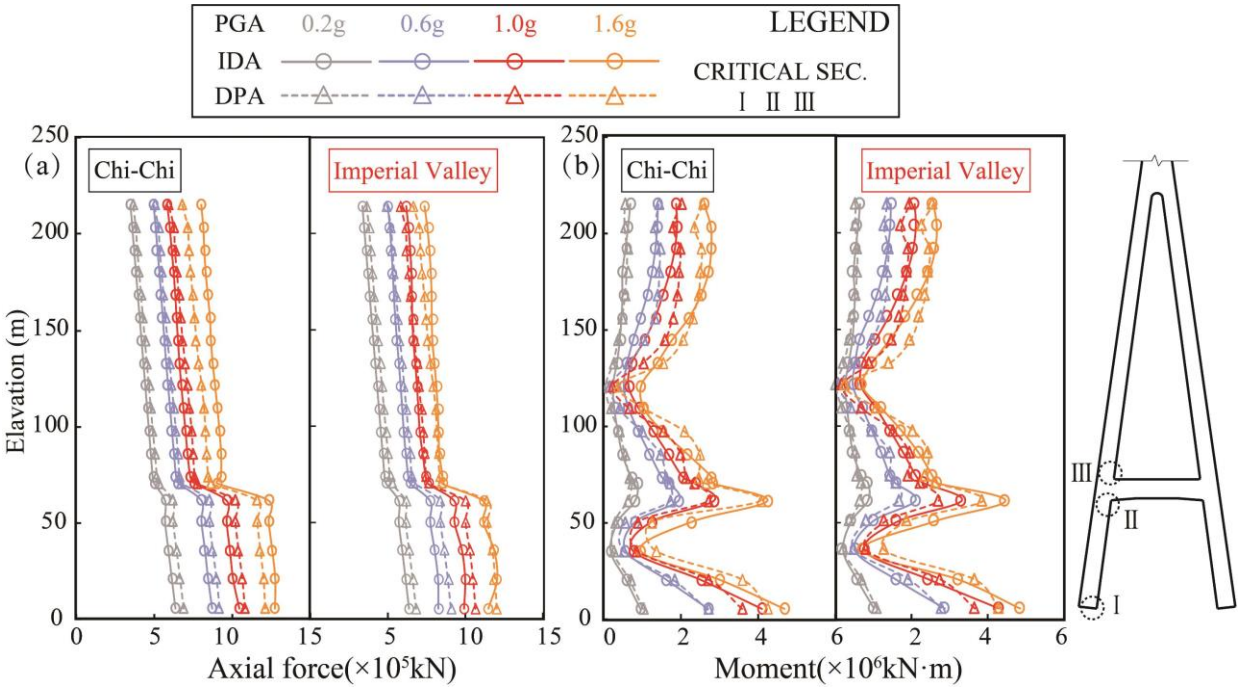

Fig.6–Axial force (a) and Moment (b) envelope distribution of the bridge tower from IDA and DPA

4.3 Detecting the occurrence/development of plastic regions along the tower

Curvature is an appropriate demand parameter for quantifying yielding states of section [23], thereby employed to detect plastic regions of the tower. Yield curvature of the critical sections can be easily obtained by Moment-Curvature analyses. It should be noted that under lateral loads (e.g., IDA and DPA), axial forces in columns of the studied inverted Y-shape RC tower keep changing. More specifically, the two columns act as leading and trailing ones by turns under IDA, while under DPA one column remains the leading one and the other remains the trailing one. Considering the impact of axial force is negligible for the capture of yield curvature [24], the yield curvature under constant gravity loads is employed in the judgement of the occurrence of plastic hinges for simplicity. When it turns to the capture of ultimate curvature, on the contrary, the variation of axial force is a significant source [24], thus requiring huge efforts in the judgement of ultimate-states in IDA and DPA. In this regard, the ultimate states are represented by the concrete core crushing, rebar snapping, or the section lateral strengths descended by 15% of their peak values, whichever occurs first. The capability of capturing the ultimate-state of the tower by IDA and DPA is discussed later in this paper.

Fig.7 compares envelope distributions of curvature and the development of plastic regions between IDA and DPA with increasing PGA from 0.2g to 1.6g. Table 2 lists the curvature captured by IDA and DPA and their errors under PGA of 0.2g, 0.6g, 1.0g and 1.6g. Table 3 lists the peak displacement of the tower when the critical sections initially yield. From Fig.7(a) and Table 2, it can be concluded that DPA can reasonably capture curvature responses in the view of engineering practice, with errors mostly within 30% for Chi-Chi and Imperial Valley motions, across the concerned PGA range. According to Fig.7(b) and Table 3, DPA is capable of detecting the yield states of critical sections and tracing the development of plastic regions. Precisely, no more than 22% error is detected when DPA is adopted to capture the initial yield-state of SECs. II and III. As for SEC. I, the error increases up to 38%. Apart from that, the initial yield-state of SEC. II is firstly detected by DPA instead of IDA, while opposite results are witnessed when it comes to SECs. I and II. It worth noting that there is a minor difference in the occurrence order and extension of plastic hinges

between IDA and DPA. For IDA, plastic hinges are firstly detected at the bottom of upper column (SEC. III), then successively at the bottom of lower column (SEC. I), finally at top of lower column (SEC. II). For DPA, SEC. III is also witnessed firstly entering yield-state, followed by SEC. II and I in order, which is contrary to DPA. Regarding the location of plastic regions, the DPA results coincide reasonably well with the IDA reference results.

Table 1 – Axial force and bending moment in critical sections from IDA and DPA

Type	Section	PGA	Chi-Chi			Imperial Valley		
			IDA	DPA	ERR	IDA	DPA	ERR
Axial force (×10^{5}kN)	I	0.2g	6.4	6.9	-8%	6.4	6.8	-7%
		0.6g	8.7	9.2	-6%	8.3	9.1	-10%
		1.0g	10.5	10.8	-3%	9.9	10.7	-7%
		1.6g	12.8	12.2	5%	11.5	12	-4%
	II	0.2g	5.8	6.3	-9%	5.7	6.2	-8%
		0.6g	8.1	8.6	-7%	7.7	8.4	-8%
		1.0g	9.7	10.2	-5%	9.3	10	-8%
		1.6g	12.4	11.7	6%	11.2	11.4	-2%
	III	0.2g	5.1	5.3	-5%	4.9	5.3	-7%
		0.6g	6.6	6.8	-3%	6.5	6.7	-3%
		1.0g	7.7	7.8	-2%	7.6	7.6	0%
		1.6g	9.1	8.7	5%	8.6	8.5	1%
Bending moment (×10^{5}kN·m)	I	0.2g	9.4	10.3	-9%	10.2	10.7	-5%
		0.6g	27	26.9	0%	28.8	27.9	3%
		1.0g	40.9	35.8	13%	43	36.8	14%
		1.6g	46.7	42.3	9%	48.5	43	11%
	II	0.2g	8.1	6.3	22%	8.6	6.4	25%
		0.6g	19.2	17	12%	21.1	17	19%
		1.0g	28.5	27.1	5%	33.1	27.2	18%
		1.6g	42.2	40.4	4%	44.6	38.9	13%
	III	0.2g	8.7	7.3	16%	8.6	6.7	22%
		0.6g	16.9	17.2	-2%	15.9	16.2	-2%
		1.0g	23.7	23.5	1%	23.1	22.3	3%
		1.6g	28.2	26.2	7%	26.7	26.6	1%

ERR= (IDA-DPA) / IDA, the same hereinafter

4.4 Force-displacement relationship

Fig.8 displays the force-displacement curves for IDA and DPA, where “force” represents the sum of horizontal shear at the bottom of two lower columns and the “displacement” refers to the peak displacement of the tower. Initial yield-states of all critical sections and ultimate-states of the tower are also labeled in Fig.

8 to show the failure mechanism difference between IDA and DPA. Inconsistent with IDA results, a significant stiffness deterioration happens in DPA after the plastic region firstly detected, eventually leading

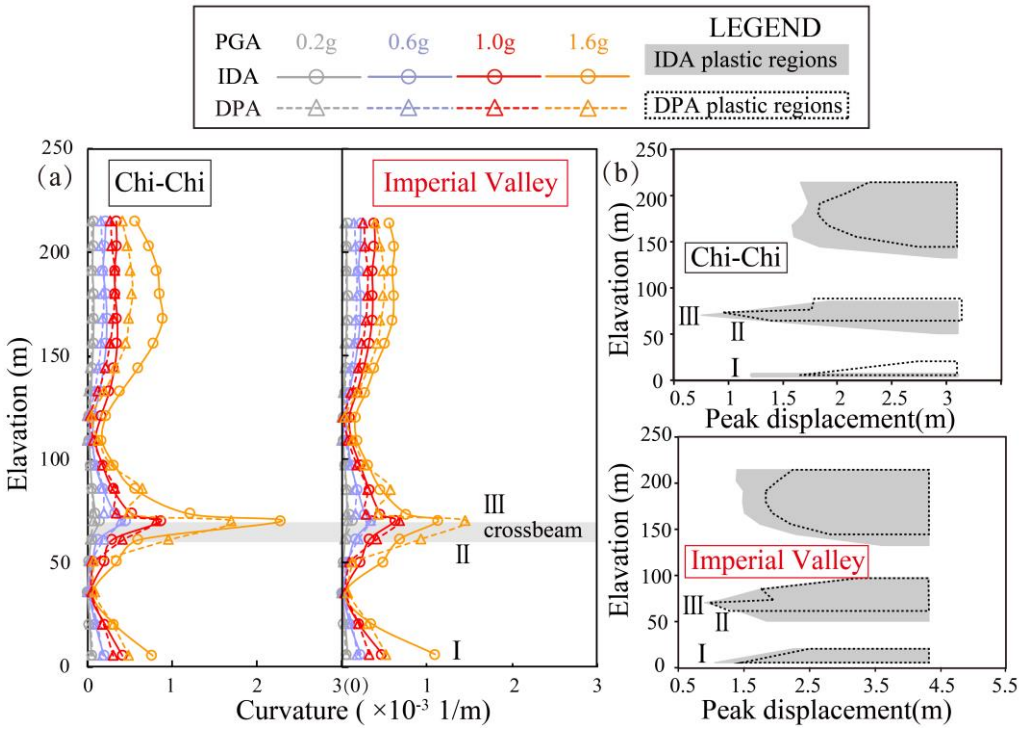

Fig. 7– Comparison of IDA and DPA results: (a) envelope distributions of curvature subjected to Chi-Chi and Imperial Valley with the PGA of 0.2g, 0.6g, 1.0g and 1.6g; (b) the development process of plastic hinges with increasing peak displacements of the tower.

Table 2 –The curvature of major plastic regions captured by IDA and DPA at the same PGA (Unit:×10^{-5} 1/m)

Section	PGA	Chi-Chi			Imperial Valley		
		IDA	DPA	ERR	IDA	DPA	ERR
I	0.2g	5.3	6.7	-28%	6.0	7.1	-19%
	0.6g	20.1	18.1	10%	23.3	19.5	16%
	1.0g	41.5	30.7	26%	48.5	32.9	32%
	1.6g	77.0	49.4	36%	111.1	53.0	52%
II	0.2g	5.3	3.9	27%	5.8	4.0	30%
	0.6g	13.3	19.8	-48%	16.5	20.5	-24%
	1.0g	29.8	42.6	-43%	33.7	42.0	-25%
	1.6g	60.7	96.7	-59%	69.2	93.9	-36%
III	0.2g	14.9	8.0	46%	13.8	7.3	47%
	0.6g	45.1	40.5	10%	35.3	34.3	3%
	1.0g	86.8	82.3	5%	63.2	68.6	-8%
	1.6g	228.7	171.1	25%	115.1	147.7	-28%

to a 15% decrease of shear force to reach the ultimate-state. Table 4 lists ductile indexes of the tower obtained by IDA and DPA. It can be concluded that DPA provides comparatively conservative results in

Table 3 –The peak displacement of the tower when critical sections initially yield (Unit: m)

Input	Section	IDA	DPA	ERR
Chi-Chi	I	1.22	1.62	-33%
	II	1.64	1.32	20%
	III	0.75	0.92	-22%
Imperial Valley	I	1.06	1.46	-38%
	II	1.43	1.26	11%
	III	0.90	0.97	-8%

terms of horizontal strength and displacement ductility factors (ultimate displacement divided by initial yield displacement) of the tower. To be precise, the horizontal strength obtained by DPA is only approximately 80% of the IDA results, and the displacement ductility obtained in DPA are 23% (Chi-Chi) and 43% (Imperial Valley) less than those in IDA. These differences are attributed to two inherent limitations of DPA. Firstly, the critical three sections are always concentrated in the trailing column in the push direction of DPA and they remain yield until the ultimate-state is reached, while in IDA two columns take turn to act as the leading and trailing ones, thereby plastic hinges may not always occur on the same column. Therefore, the IDA results do not show a significant deterioration of stiffness. The other reason is that the load pattern of DPA may not be rational when the structure significantly enters post-yield state as the Equal Displacement Principle is not well followed anymore.

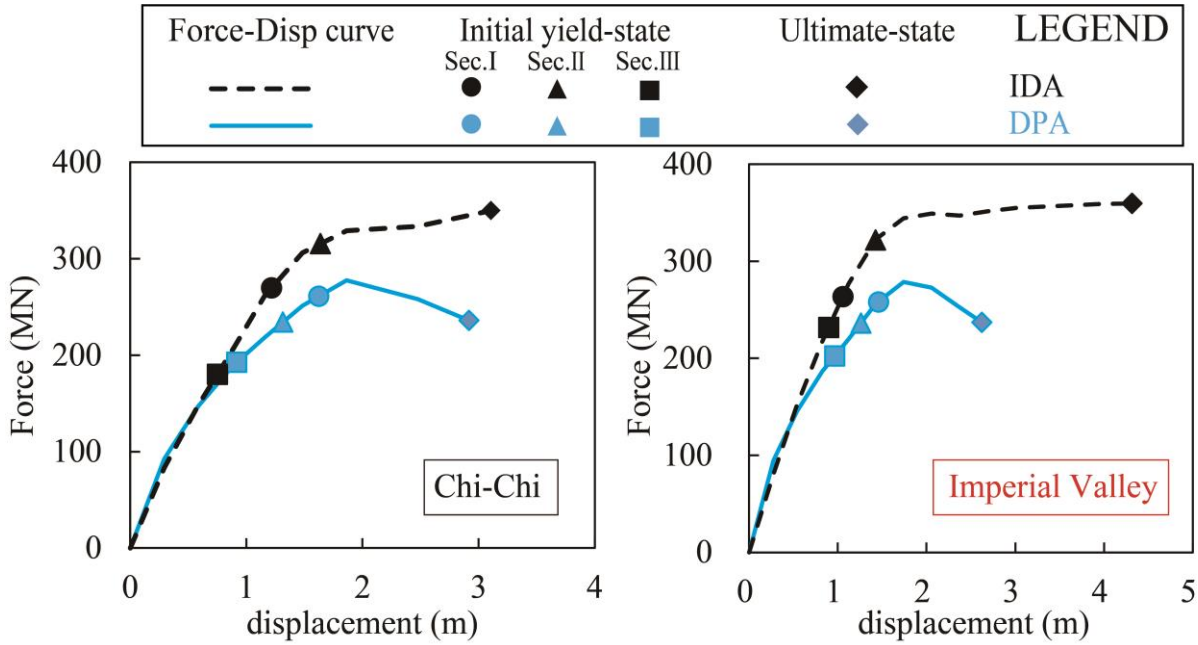

Fig. 8–The force-displacement curves for IDA and DPA

In addition, it is worth mentioning that DPA has an overwhelming advantage over IDA in computational efficiency. In a computer with CPU @3.2GHZ and 8GB RAM, it takes as many as 32 hours to accomplish all nonlinear time-history analyses in IDA while in DPA only 30 seconds are needed for the pushover analyses. Apparently, DPA is more efficient when a complex nonlinear structure, like long-span bridge tower, is involved.

Table 4 –Ductile indexes of the tower obtained by IDA and DPA

Input	Method	Peak shear force/MN (1)	Peak disp of the tower when initially yield/m (2)	Ultimate peak disp of the tower /m (3)	Disp ductility factor (3)/(2)
Chi-Chi	IDA	350	0.75	3.11	4.15
	DPA	278	0.92	2.92	3.17
Imperial Valley	IDA	359	0.90	4.32	4.80
	DPA	279	0.97	2.62	2.70

5. Conclusions

A deformation-based pushover analysis (DPA) method is proposed in this paper to efficiently obtain transverse seismic demands and investigate the seismic failure mechanism as well as ductility of RC tower for long span cable-stayed bridge. Based on a real kilometer-span cable-stayed bridge, elastic full-bridge and equivalent single tower FE model are built to perform IDA and DPA respectively using two typical ground motion records. The proposed DPA is validated by comparing the axial force, moment, plastic region development, the force-displacement relationship of the tower between IDA and DPA. Inherent limitations of the proposed DPA are pointed out as well. Main findings are as follows.

(1) The proposed DPA method is capable of providing estimation on axial forces, bending moments, and occurrence/development of plastic regions of RC towers with acceptable accuracy for engineering practice.

(2) Considering the inherent limitations of DPA, horizontal strengths of RC towers and ultimate displacements are always conservatively predicted by DPA (approximately as larger as 80%) as compared to IDA.

(3) DPA is highly computationally efficient and easy for application in preliminary estimates of seismic behavior of RC towers.

6. Copyrights

7. References

[1] Ministry of Communications of the People's Republic of China (2008): Guidelines for Seismic Design of Highway Bridges. Beijing, China.

[2] American Association of State Highway and Transportation Officials (AASHTO) (2012):AASHTO LRFD bridge design specifications. 6th ed. Washington, D.C.

[3] Japan Society of Civil Engineering (JSCE) (2005): Standard specifications for concrete structures-2002: seismic performance verification.

[4] Calvi GM, Sullivan TJ, Villani A (2010): Conceptual seismic design of cable-stayed bridges. *Journal Of Earthquake Engineering*, 14(8), 1139–1171.

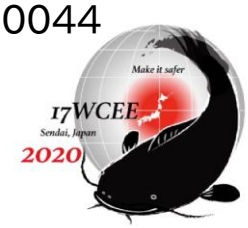

[5] Loh C-H, Tsay C-Y (2001): Responses of the earthquake engineering research community to the Chi-Chi (Taiwan) earthquake. *Earthquake Spectra*,;17(4), 635–656.

[6] Chadwell CB, Fenves GL, Mahin SA (2003): Near Source Earthquake Effects on the Ji Lu Cable-stayed Bridge in the 21 September 1999 Chi-Chi Taiwan Earthquake. University of California, Berkeley.

[7] Bertero V.V (1977): Strength and deformation capacities of buildings under extreme environments. *Structural Engineering & Mechanics*: 53(1), 211-215.

[8] Vamvatsikos D, Cornell CA (2002): Incremental dynamic analysis. *Earthquake Engineering and Structural Dynamics*, 31(3), 491–514.

[9] Chopra, A. K., and Goel, R. K. (2002): Modal pushover analysis procedure for estimating seismic demands for buildings, *Earthquake Engineering and Structural Dynamics*, 31 (3), 561–582.

[10] Chopra, A. K., and Chintanapakdee, C. (2004): Evaluation of modal and FEMA pushoveranalyses: Vertically ‘‘regular’’ and irregular generic frames, *Earthquake Spectra,* 20 (1), 255–271.

[11] Bracci JM, Kunnath SK, Reinhorn AM (1997): Seismic performance and retrofit evaluation of reinforced concrete structures. *Journal of Structural Engineering ASCE*, 123(1), 3–10.

[12] Gupta B, Kunnath SK (2000): Adaptive spectra-based pushover procedure for seismic evaluation of structures. *Earthquake Spectra*, 16(2), 367–391.

[13] Antoniou S, Pinho R (2004): Development and verification of a displacement-based adaptive pushover procedure. *Journal of Earthquake Engineering,* 8(5), 643–661.

[14] Miranda E (2000): Inelastic displacement ratio for structures on firm sites. *Journal of Structural Engineering ASCE*, 126(10), 1150-1159.

[15] Riddel R, Hidalgo P, Cruz E (1989): Response modifaction factors for earthquake resistant design of short period structures. *Earthquake Spectra*, 5(3), 571-590.

[16] Araujo, M, Delgado, R (2011): Seismic behaviour modelling of strutures using sap2000. *International Conference on Recent Advances in Nonlinear Models - Structural Concrete Applications*, Coimbra, Portugal.

[17] McKenna F (2011): OpenSees: a framework for earthquake engineering simulation. *Computer in Science and Engineer*, 13(4), 58–66.

[18] Wang, X., Fang, J., Zhou, L., and Ye, A. (2019): Transverse seismic failure mechanism and ductility of reinforced concrete pylon for long span cable-stayed bridges: Model test and numerical analysis. *Engineering Structures*, 189, 206–221.

[19] Zhou L, Wang X, Ye A. (2019): Shake table test on transverse steel damper seismic system for long span cable-stayed bridges. *Engineering Structures*, 179, 106–119.

[20] Ye A. ,Zhou L, Cheng G, Wang X (2018): Lateral quasi-static test of inverted Y-shaped concrete tower for long span cable-stayed bridges, *China Civil Engineering Journal*, 51(9), 67-73.

[21] Earthquake Administration of Jiangsu Province (2000): Seismic Design Parameters for Ground Motion Inputs. Seismic Safety Evaluation of Site of Sutong Bridge, Nanjing, China.

[22] Power M, Chiou B, Abrahamson N, Bozorgnia Y, Shantz T, Roblee C (2008): An overview of the NGA project. *Earthquake Spectra*, 24(1), 3–21.

[23] Wang, X., Shafieezadeh, A., and Ye, A.(2019): Optimal EDPs for post-earthquake damage assessment of extended pile-shaft–supported bridges subjected to transverse spreading. *Earthquake Spectra*, 35(3), 1367–1396.

[24] Wang, X., Ye A., and Shang Y.(2016): Quasi-Static Cyclic Testing of Elevated RC Pile-Cap Foundation for Bridge Structures, *Journal of Structural Engineering ASCE*, 21(2), 04015042.

